Electron transport through planar defects: a new description of grain boundary scattering

1991 J. Phys.: Condens. Matter 3 6989

(http://iopscience.iop.org/0953-8984/3/36/004)

J. Phys.: Condens. Matter 3 (1991) 6989–6999. Printed in the UK

Electron transport through planar defects: a new description of grain boundary scattering

A Knäbchen
Institut für Theoretische Physik der Technischen Universität Chemnitz, Reichenhainer Strasse 70, Chemnitz, D-9010, Federal Republic of Germany

Received 4 March 1991

Abstract. Based on a recently developed superposition method, the resistance of a homogeneous bulk material perturbed by a planar defect is calculated. A detailed analysis of the evolving residual-resistivity dipole surrounding the layer is given. Transmission and reflection of attenuated propagating waves on planar defects describe the essential features of grain boundary scattering. In this connection our result can be compared with experimental data and well known theories on polycrystalline metals.

1. Introduction

Electronic transport in materials containing defects is accompanied by strong inhomogeneities in the microscopic electric field and the carrier density. For the first time Landauer studied the nature of these inhomogeneities. In his 1957 paper [1] he pointed out that the transport field arising from a scatterer is a highly localized dipole field called the residual-resistivity dipole (RRD). The formation of the RRD is the microscopic mechanism which yields the voltage drop across the scatterer. For a one-dimensional (1D) system, a careful investigation leads straightforwardly to the well known Landauer formula (LF) [1, 2]. This formula predicts a resistance proportional to $R/(1-R)$ where R is the reflection coefficient of the scatterer.

Besides localized scatterers in the 1D and 3D bulk, in his paper mentioned above, Landauer considered the influence of planar defects on the electronic flow. On the one hand, this problem corresponds closely to the simpler case of a perturbation in a 1D system because the electrons cannot detour around the scattering obstacle. It can be shown, cf below, that such behaviour causes a denominator $(1-R)^{-1}$ in the resistance, quite similar to the LF. On the other hand, the treatment of carriers propagating in the 3D bulk is more complicated and constitutes a step towards experimentally realized situations. For instance, contact resistances can be considered as an example of partly reflecting planar perturbations [3].

Planar defects are widely used as a simplified model system for grain boundaries. Their description by smooth and short-range potentials seems to be justified [4]. As far as we know, all calculations concerning grain boundaries have been carried out on the basis of classical or semiclassical transport concepts, i.e. the Boltzmann equation has been complemented by an independently determined collision or source term [4–8]. The authors of [4–7] have calculated a collision term and a corresponding relaxation time. The deviations of the different approaches are more or less a matter of taste and characterize the difficulties arising from a semiclassical hybrid treatment of localized perturbations. Especially the combination of both grain boundary scattering and uniform background scattering to an effective mean free path or relaxation time requires additional assumptions that cannot be proved within the scope of a classical theory. Finally we note that the results mentioned do not confirm Matthiessen's rule, according to which the total resistance should be the sum of all individual resistances, i.e. (here) of a bulk and a grain boundary contribution. On the contrary, our result does satisfy Matthiessen's rule (cf the discussion).

The treatment of the grain boundary by Sorbello [8] is related more closely to the original ideas of Landauer. He considers an impurity layer or grain boundary, sandwiched between reservoirs, and gives its resistance for a weakly scattering layer. His local-field method employs different concepts for the near- and far-field regions. A carrier density perturbation due to the quantum-mechanical scattering of electrons at the grain boundary describes the near-field region. For $r \gg l$, where l is the mean free path (MFP) in the bulk, a Boltzmann equation completed by a source term is solved. In the source term the information on the location of the layer is retained whereas the conventional transport approach uses only the ensemble-averaged transition probability in the collision term.

Our method to handle the problem is different from all these [1, 4–8] and has the advantage that the interplay between coherent propagation and incoherent transport away from the defect are incorporated simultaneously. Thus our method, which we call the superposition method (SPM), connects both processes already included in the local-field method and puts them on a unified mathematical basis. In the following we shall use the SPM in its recently developed approximate form. This formalism is an appropriate tool for systems where, in principle, an obstacle of arbitrary strength, shape and size is superimposed on a weakly scattering background, i.e. the MFP l within the ensemble of disordered background scatterers is large compared with the wavelength λ of electrons. The smallness of the parameter λ/l is the main assumption for the validity of the SPM applied. For good bulk conductors, e.g. metals, $\lambda/l \ll 1$ holds.

Concerning the problem under consideration, the only condition that we set is that the width of the layer is small compared with the MFP. This permits later on an essential mathematical simplification. Because of the proposed weak background, however, the layer need not be thin on the λ scale.

It is worth emphasizing that the defect plane is allowed to scatter the electron waves strongly. The possibility of treating strongly reflecting walls is a substantial improvement and makes a perturbational treatment [4] or similar ideas [5] superfluous. Some work [4–6] is practically limited from the very beginning to weakly scattering defects although the corresponding resistivity formulae have been evaluated in the whole range. On the basis of Landauer's results [1] for a 1D system one expects here a solution characterized by the $R/(1-R)$ structure, too. Even for a strong defect the existence of an enhancement factor $(1-R)^{-1}$ and its exact form can be derived. Hence we are able to generalize Sorbello's result in this respect.

The SPM can be applied to the mobility case with a driving force or to the diffusion case with a constant carrier density gradient. The latter is mathematically much simpler and will be used in the following. This decision is only a formal matter because it is well known how to go from diffusivity to conductivity via the Einstein equivalence. For a point-like impurity both cases have been treated in parallel and compared in detail [9].

In section 2 a short summary of the SPM, adjusted to our purposes, is given based on a more detailed explanation in [2]. In sections 3 and 4 we construct, in a two-step procedure, the solution in the diffusion picture. Then, in section 5, we perform the transformation from the diffusion to the force case, i.e. the density pile-up surrounding the planar defect passes into a voltage drop. For a granular material consisting of grains with a mean size or diameter D, the resulting conductivity will be determined on the condition that $D \gg l$ where our solution for a single grain boundary is not affected by the presence of other ones. A comparison of our formula with results already known is made. Further discussion is given in section 6.

2. Superposition method

A stationary diffusion current in a homogeneous bulk material is related to a constant carrier density gradient. Under the combined action of current flow and additional perturbation, the density $\rho(\boldsymbol{r})$ can be expressed according to [2] as $\rho(\boldsymbol{r}) = \bar{\rho}(\boldsymbol{r}) + \delta\rho(\boldsymbol{r})$. The carrier distribution $\bar{\rho}$ has the property

$$\frac{\partial}{\partial \boldsymbol{r}}\left(\frac{\bar{\rho}(\boldsymbol{r})}{\operatorname{Im} G(\boldsymbol{r},\boldsymbol{r})}\right) = \text{const} \equiv \boldsymbol{g}. \tag{1}$$

Far from the obstacle the density gradient reaches a given value, grad ρ, and the density of states, which is proportional to Im $G(\boldsymbol{r},\boldsymbol{r})$, approaches its unperturbed bulk value. Hence, $\boldsymbol{g}$ is given by grad $\rho/\operatorname{Im} G_{\mathrm{b}}$ and the part $\bar{\rho}$ yields already the asymptotically correct density gradient. Therefore, $\delta\rho(\boldsymbol{r})$ represents the current-induced carrier redistribution due to the obstacle. This latter part obeys in the same approximation as in [2] an integral equation

$$\delta\rho(\boldsymbol{r}) = \rho_{\mathrm{ind}}(\boldsymbol{r}) + (\operatorname{Im} k^2/\operatorname{Im} G_{\mathrm{b}}) \int \mathrm{d}^3r'\, |G(\boldsymbol{r},\boldsymbol{r}')|^2\, \delta\rho(\boldsymbol{r}'). \tag{2}$$

G is the one-particle Green function in a simple medium approximation

$$[\Delta + k^2 - (2m/\hbar^2)V(\boldsymbol{r})]G(\boldsymbol{r},\boldsymbol{r}') = -\delta(\boldsymbol{r}-\boldsymbol{r}') \tag{3}$$

where $k = k' + \mathrm{i}k''$ denotes the medium wavenumber. Its imaginary part $k'' = (2l)^{-1}$ follows from the disordered background scatterers and is responsible for the attenuation of the coherent wave field [10]. In equation (3) the potential $V(\boldsymbol{r})$ describes quite generally an obstacle and/or a confinement disturbing the propagation process. For convenience, $G = G_{\mathrm{b}} + G_{\mathrm{sc}}$ is decomposed into an unperturbed bulk term $G_{\mathrm{b}}(\boldsymbol{r},\boldsymbol{r}') = \exp(\mathrm{i}k|\boldsymbol{r}-\boldsymbol{r}'|)/(4\pi|\boldsymbol{r}-\boldsymbol{r}'|)$ and a scattering part G_{sc}.

The scattering of electrons incident at an obstacle or defect produces a current-induced coherent density change $\rho_{\mathrm{ind}}(\boldsymbol{r})$, which reads

$$\rho_{\mathrm{ind}} = \rho_1 + \rho_2$$

with

$$\rho_1(\boldsymbol{r}) = 2\boldsymbol{g} \int \mathrm{d}^3r' \operatorname{Im}\left(G^*_{\mathrm{sc}}(\boldsymbol{r},\boldsymbol{r}')\frac{\partial}{\partial \boldsymbol{r}'}G_{\mathrm{b}}(\boldsymbol{r},\boldsymbol{r}')\right) \tag{4a}$$

$$\rho_2(\boldsymbol{r}) = \mathrm{i}\boldsymbol{g} \int \mathrm{d}^3r'\, G_{\mathrm{sc}}(\boldsymbol{r},\boldsymbol{r}')\frac{\partial}{\partial \boldsymbol{r}'}G^*_{\mathrm{sc}}(\boldsymbol{r},\boldsymbol{r}'). \tag{4b}$$

Since ρ_{ind} is subject to a multiple scattering process in the bulk, which destroys phase relations, the coherent density is attenuated and localized within a few MFP around the defect. Corresponding to equation (2), ρ_{ind} acts as an initial distribution for a classical transport process to follow. Asymptotically, this is classical diffusion [11]. However, only the pure bulk term $|G_{\mathrm{b}}|^2$ in the integral on the right-hand side of (2) is responsible for the long-range behaviour of the diffusive solution $\delta\rho(\boldsymbol{r})$. Nevertheless, there are two further contributions with G_{sc} or $|G_{\mathrm{sc}}|^2$, respectively. Thus a defect acts twofold: it yields a coherent density perturbation and influences the following diffusion process.

Finally we notice that in (2) and (4) the regions of the added defect can be neglected in the integrals over $\boldsymbol{r}'$. This approximation is justified because the MFP determines the length scale of the regions that contribute significantly. As noted above, the width of the layer should be small compared with l. If we neglect the waves emerging primarily from that region we have, in principle, no background scatterers within the obstacle.

To summarize, one can say that the SPM divides the problem into two separated ones: determination of the coherent density change (4) occurring in the vicinity of the defect and solution of a modified transport problem (2), which yields a delocalized diffusive behaviour of the total density redistribution $\delta\rho$. The next two sections are devoted to them.

3. Induced density

3.1. Green function G_{sc}

We use cylindrical coordinates (R, φ, z), where the z axis is normal to the planar defect. Since the scattering potential is independent of R and φ, and non-zero within a layer (around $z = 0$) only, the scattering properties can be specified in terms of coefficients $R(\theta)$ and $T(\theta)$ for specular reflection and transmission, respectively. (To avoid potential misunderstanding the reflection coefficient $R(\theta)$ is written with an argument, at least when the coordinate R appears.) Here θ is the angle of incidence, and $R(\theta) + T(\theta) = 1$. If we choose $\boldsymbol{r}$ on the z axis, i.e. $R = 0$, the Green function G_{sc} can be written outside the defect as

$$G_{\mathrm{sc}}(\boldsymbol{r}, \boldsymbol{r}') = [t(\theta_-) - 1]G_{\mathrm{b}}([R'^2 + (z - z')^2]^{1/2}) \equiv [t(\theta_-) - 1]G_{\mathrm{b}}^- \tag{5a}$$

for $\mathrm{sgn}(z) \neq \mathrm{sgn}(z')$ and

$$G_{\mathrm{sc}}(\boldsymbol{r}, \boldsymbol{r}') = r_{l,r}(\theta_+)G_{\mathrm{b}}([R'^2 + (z + z')^2]^{1/2}) \equiv r_{l,r}(\theta_+)G_{\mathrm{b}}^+ \tag{5b}$$

for $\mathrm{sgn}(z) = \mathrm{sgn}(z')$, where $|t(\theta)|^2 = T(\theta)$ and $|r_{l,r}(\theta)|^2 = R(\theta)$. The amplitudes $r_{l,r}$ characterize reflection from the left-hand or right-hand side of the potential. The angle is given by $\cos\theta_\pm = (z \pm z')/[R'^2 + (z \pm z')^2]^{1/2}$. The Green function G_{sc} in (5a) corresponds to transmitted waves propagating from a point $\boldsymbol{r}$ to point $\boldsymbol{r}'$. The Green function G_{sc} in (5b) describes the reflection case where a fictitious mirror source at the point $-\boldsymbol{r}$ appears.

Outside the potential sheet G_{sc} obeys the homogeneous wave equation $(\Delta + k^2)G_{\mathrm{sc}} = 0$ (cf (3)). It can be shown that our solution (5) fulfils it up to higher-order terms in $\{k'[R'^2 + (z \pm z')^2]^{1/2}\}^{-1}$, which are negligible in the relevant region.

3.2. *Calculation of the induced density*

The Green functions G_b and G_{sc} are independent of the variable φ. Hence, only the z component of the derivative yields non-vanishing terms in (4). We employ the approximation

$$\frac{\partial}{\partial z'} G_{sc/b} \approx \pm i k' \cos\theta_{\pm} \, G_{sc/b} \tag{6}$$

for $k'[R'^2 + (z \pm z')^2]^{1/2} \gg 1$, suppressing the small imaginary part k'', too. The induced density part ρ_1 is now given by

$$\rho_1 = -2k'\boldsymbol{g}\cdot\hat{\boldsymbol{z}}\,\mathrm{Re}\int \mathrm{d}A' \int_{+/-} \mathrm{d}z' \begin{Bmatrix} r^*_{l,r}(\theta_+) \\ t^*(\theta_-) - 1 \end{Bmatrix} (G_b^{\mp})^* \cos\theta_- \, G_b^- \tag{7}$$

where $\int_{+/-} \mathrm{d}z' \ldots$ is restricted to values z' with $\mathrm{sgn}(z')$ equal/unequal to $\mathrm{sgn}(z)$ and $\int \mathrm{d}A' = \int \mathrm{d}R'\, R'\, \mathrm{d}\varphi'$. Besides the phase compensating term $|G_b^-|^2$ in equation (7) there is an oscillatory interference term $\sim r^*(G_b^+)^* G_b^-$ due to the reflected waves. Its very existence is a consequence of our non-classical procedure, although it causes only density corrections localized within some wavelengths around the defect and is therefore negligible compared with the smoth contributions. Remember that in the corresponding 1D case with a scatterer the oscillatory density terms dominate the near-field region ($|z| \lesssim l$) for a weak scatterer [2]. Generally they are irrelevant for all integral features, especially for the induced dipole moment, which determines the asymptotic solution of the diffusion process. The difference between the grain boundary and the 1D case emphasizes the significance of dimension.

With the remaining part of (7) and ρ_2 we immediately obtain

$$\rho_{\mathrm{ind}}(z) = 2k'\boldsymbol{g}\cdot\hat{\boldsymbol{z}} \int \mathrm{d}A' \int_+ \mathrm{d}z' \, |G_b^+|^2 \cos\theta_+ \, R(\theta_+) \tag{8}$$

or, after integration over z',

$$\rho_{\mathrm{ind}}(z) = 2k'l\boldsymbol{g}\cdot\hat{\boldsymbol{z}}\,\mathrm{sgn}(z) \int_{(z'=0)} \mathrm{d}A' \, |G_b|^2 R(\theta) \cos^2\theta .$$

The latter formula is very suggestive. In case of current flow, each point on the defect sheet acts as a source of a spherical wave. The superposition of their intensities weighted by the reflection coefficient yields the coherent density. The product $\mathrm{d}A' \cos\theta$ measures the effective area of radiation for each angle θ. We note that such a $\cos\theta$ dependence is known as Lambert's law [17]. The second cosine can be related in a more classical picture to the distribution function of those incident particles which form the induced current. This current is orientated in the z direction and redistributes carriers around the planar defect generating the coherent density.

According to (8) there exists a density pile-up in front of the layer and a deficiency behind it, forming the typical coherent density dipole. This agrees exactly with the concept one has in mind if a current is hindered by an obstacle. Owing to the scalar product between the density gradient ($\sim \boldsymbol{g}$) and the normal vector $\hat{\boldsymbol{z}}$, ρ_{ind} depends on the direction of current flow. Particularly, there is no effect when current and planar defect are parallel to each other in accordance with the presupposed specular reflection.

Consider the asymptotic behaviour, $|z| \gg l$. Contrary to the near-field region where nearly all angles contribute, the induced density is now given by

$$\rho_{\mathrm{ind}}(z) \simeq l \,\mathrm{grad}\, \rho \cdot \hat{z}\, \mathrm{sgn}(z) R(0)(l/|z|) \exp(-|z|/l) \tag{9}$$

to the lowest order of $l/|z| \ll 1$. Besides the exponential attenuation, ρ_{ind} decreases as $|z|^{-1}$ because for larger distances from the defect only waves in a narrow cone around $\theta \simeq 0$ reach point $\boldsymbol{r}$ with notable amplitudes. Consequently, the reflection coefficient for normal incidence, $R(0)$, governs the coherent field. This different behaviour in the near and far regions is a feature of the planar arrangement.

In the next section we will need the dipole moment of the induced density. It reads with (8)

$$p_{\mathrm{ind}} = \int_{-\infty}^{+\infty} \mathrm{d}z\, z \rho_{\mathrm{ind}}(z) = l^3 \,\mathrm{grad}\, \rho \cdot \hat{z} \int_{-1}^{1} \mathrm{d} \cos\theta\, |\cos^3\theta| R(\theta) \tag{10}$$

where the mentioned dominance of small angles is revealed in a higher power of $\cos\theta$.

4. Total density

With regard to the potential drop across the layer we are only interested in the asymptotic solution of the integral equation. Since our *ansatz* $\bar{\rho}$ already yields the required density gradient the total density has to be asymptotically ($|z| \gg l$) a dipole distribution, namely

$$\delta\rho(z) \simeq C\, \mathrm{sgn}(z) \tag{11}$$

where C is an unknown constant. We remark that in contrast to the 1D and 3D systems with an added scatterer [2], $\delta\rho$ (11) does not correspond to the induced density (9) without a damping factor. The evaluation of C via Fourier transformation is straightforward because the oscillatory term $(G_{\mathrm{b}}^{+})^{*} G_{\mathrm{b}}^{-}$ in the integral kernel in (2) can be neglected (cf discussion of equation (7)). The remaining contributions can be treated like convolution integrals. After some manipulations (see appendix) we obtain C as determined by dipole moments as follows:

$$C = p_{\mathrm{ind}}/p\left[\mathrm{sgn}(z) - \int \mathrm{d}^3 r' |G(\boldsymbol{r}, \boldsymbol{r}')|^2 \,\mathrm{sgn}(z')\right] \tag{12}$$

where $p[\ldots] = \int_{-\infty}^{\infty} \mathrm{d}z\, z[\ldots]$ denotes the calculation of the dipole moment. Combining equations (11) and (12), and the induced dipole moment (10), we finally get the total density in the far-field region as

$$\delta\rho(z) \simeq l \,\mathrm{grad}\, \rho \cdot \hat{z}\, \mathrm{sgn}(z) \int_{-1}^{1} \mathrm{d}\cos\theta\, |\cos^3\theta|\, R(\theta) \Big/ \int_{-1}^{1} \mathrm{d}\cos\theta \cos^2\theta\, T(\theta). \tag{13}$$

The density difference between both sides of the layer or grain boundary is given by

$$|\Delta\rho| = 2l\, |\mathrm{grad}\, \rho \cdot \hat{z}|\, \mathfrak{R}/\mathfrak{T} \tag{14}$$

where $\mathfrak{R}$ and $\mathfrak{T}$ represent the angle integrals over $R(\theta)$ and $T(\theta)$, respectively, according to equation (13). We emphasize that $\Delta\rho$ is superimposed on the bulk density gradient and associated with the extra resistance due to the planar defect, cf next section.

Our result (14) yields the density pile-up caused by the defect and generalizes the solution of the corresponding 1D system [2]. In accordance with it and the LF the typical '$\mathfrak{R}/\mathfrak{T}$' structure is reproduced in $|\Delta\rho|$ characterizing a scattering object that cannot be circumvented by carriers. In fact, this structure guarantees immediately the correct behaviour in the two limits of very small and very large $R(\theta)$. First, for small reflection, $\Delta\rho$ has to be determined by the part R of carriers which are scattered back from the layer into the bulk. Secondly, for large reflection coefficients, the planar defect hinders to a high degree the diffusive recombination of excess and deficit carriers forming the RRD and, therefore, effects due to repeated interaction of the particles with the extended obstacle become important. In the 1D case these processes lead to a factor $(1 - R)^{-1}$ already discussed by Landauer [1] and here to the more complicated denominator in (14). The denominator ensures $|\Delta\rho| \to \infty$ for impenetrable obstacles.

The solution (14) for the density change across a planar defect can be applied to an arrangement of parallel and sufficiently separated planar defects. On condition that their mutual distance D is much greater than the MFP (or strictly speaking that $\exp(-D/l) \ll 1$) the carriers undergo during propagation between successive defects an additional scattering in the background. Such scattering events destroy the previously accumulated phase. Consequently, the planar defects in this case act on the electronic flow independently of each other. Therefore we find the resulting density pile-up simply as a multiple of the value (14). In other words, for a lattice of defects or grain boundaries with mean distance D, on average an additional density gradient appears which is proportional to $|\Delta\rho|/D$.

5. Conductivity

We now translate our result into the common picture where a current is driven by a constant electric field. According to [2], the long-range diffusion dipole (13) is related to a potential drop established within a microscopic screening length around the layer. Then, combined with the current, the extra resistance arising from a planar perturbation follows. Guided by the considerations of Lenk [2], we deduce immediately that a lattice of defects with interplanar spacing D changes the conductivity of an otherwise uniform sample to

$$\sigma/\sigma_b = [1 + 2l\mathfrak{R}\,|\cos\vartheta|/(D\mathfrak{T})]^{-1} \tag{15}$$

where $\sigma_b = e^2nl/mv$ denotes the bulk conductivity and ϑ is the angle between the current direction and the layer normal. To obtain equation (15), we have assumed a degenerate electron gas; all values are taken at the Fermi energy.

As equation (15) indicates, both scattering mechanisms contribute independently to the resistivity, i.e. there are pure bulk and defect-induced terms. The latter depends, as discussed above, linearly on the density of defects, D^{-1}. Thus we can describe the perturbed bulk with a resulting MFP, l_{eff}, according to

$$l_{\mathrm{eff}}^{-1} = l^{-1} + 2|\cos\vartheta|\mathfrak{R}/(D\mathfrak{T}). \tag{16}$$

The additivity of all individual resistivities or reciprocal MFP is sometimes called Matthiessen's rule. In contrast to a classical treatment, this rule appears here not as an assumption but as a result.

Formula (15) holds for arbitrarily strong reflecting but widely separated, $\exp(-D/l) \ll 1$, defects. These conditions are realized in coarse-grained materials.

Relevant experimental data confirm qualitatively our result [12]. We mention that for very large grains $D \to \infty$ the contribution of the grain boundaries to the resistivity becomes negligible in agreement with equation (15). In the limit of small reflection, $R(\theta) \ll 1$, we replace $T(\theta)$ in the denominator $\mathcal{T}$ by 1 and obtain

$$\frac{\sigma}{\sigma_b} = \left[1 + 6\,|\cos\vartheta| \left(\frac{l}{D}\right) \int_{-1}^{1} \mathrm{d}\cos\theta\,|\cos^3\theta|\,R(\theta)\right]^{-1}. \tag{17}$$

Note that this equation, for the special case $\vartheta = 0$, can be already derived from Sorbello's paper [8].

To compare our result with other formulae we choose the simplest case of a weak angle dependence in equation (15), $R(\theta) = 1 - T(\theta) \simeq \text{const} = R = 1 - T$, where R and T are introduced to express some average properties of the boundaries. Furthermore we set $\cos\vartheta = 1$ for a system where the electric field is applied perpendicular to parallel and planar grain boundaries and $\overline{\cos\vartheta} = 1/2$ for an isotropic polycrystalline bulk material with randomly orientated grains. Carrying out the integration over $\cos\theta$ this leads to

$$\sigma_\perp/\sigma_b = (1 + 3\alpha/2)^{-1} \qquad \alpha = lR/DT \tag{18a}$$

and

$$\sigma_i/\sigma_b = (1 + 3\alpha/4)^{-1} \tag{18b}$$

respectively. A parameter α as defined in (18) also appears in other considerations of polycrystalline metals, namely in a model proposed by Mayadas and Shatzkes (MS) [4] and in calculations performed by Warkusz (W) [6]. In figure 1 the dependence of the reduced grain boundary conductivity on α is shown according to MS (equation (10) in [4]), W (equation (16) in [6]) and equations (18). One can see that the calculated conductivities tend to the monocrystalline one if the crystal diameter or interplanar spacing D is much greater than the MFP of the electron l ($\alpha \ll 1$), and vanish if $R \to 1$ ($\alpha \gg 1$). The curves of the MS formula and equation (18a) and of the W formula and equation (18b), respectively, are similar and they have the same limiting forms for small α. However, the model developed by W cannot be related exactly to our assumption

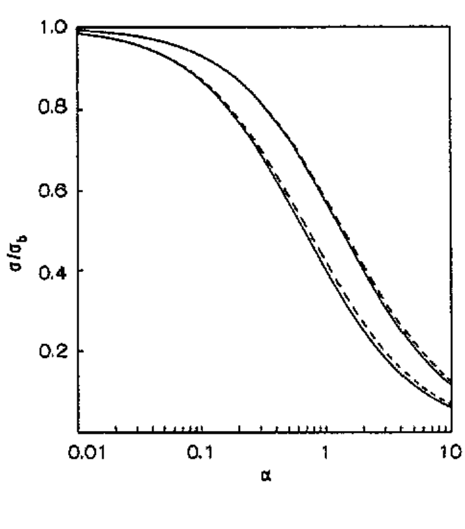

Figure 1. The reduced grain boundary conductivity σ/σ_b versus α. Broken curves: W model (upper curve), MS model (lower curve). Full curves: equation (18b) (upper curve), equation (18a) (lower curve).

leading to (18*b*) and therefore this similarity is somewhat surprising, whereas the correspondence with the MS result is not unexpected. These authors also treat the problem where a series of partially reflecting and transmitting planar grain boundaries perpendicular to the direction of the electric field act simultaneously with isotropic background scattering. In fact, the curves coincide when the grain boundary scattering is weak ($\alpha \ll 1$) but the relative deviation between the MS result and equation (18*a*) increases as T decreases. This is easy to understand by keeping in mind that the perturbation method used by MS is not valid for small T values. Nevertheless, the MS solution represents a good approximation to our expression (18*a*). We deduce that when many experiments on the conductivity of polycrystalline metal films have shown reasonable agreement with the MS model, the data can also be described by applying the proposed model, and values of the reflection and transmission coefficients can be extracted.

6. Discussion

In this paper we have dealt with the carrier density and field inhomogeneities arising from a planar defect in a current-carrying bulk material. The calculations are tractable within the framework of the superpositon method, which represents a completely formalized non-classical transport theory, and which is described in section 2. In the neighbourhood of the defect whose thickness remains small compared with the MFP within the background, an RRD appears. Its magnitude is given by equation (13) in the diffusion picture and it contains—in generalization of the LF—a quotient of angle-averaged reflection and transmission coefficients. However, in contrast to Landauer's original consideration of the 3D case [1], both coefficients have to be averaged separately. In accordance with recent scanning tunnelling microscopy (STM) experiments [13] and the former discussion by Landauer, the evolving diffusion dipole corresponds—in a charge-compensating bulk—to a voltage drop, which occurs in the immediate vicinity (within an electron screening length) of the defect plane. Founded on this solution for one defect we delivered the conductivity (equation (15)) for a series of such partially transmitting planes or grain boundaries with mean spacing D superimposed on isotropic background scattering.

The electrical resistivity σ^{-1} comprises a pure bulk term and a grain boundary contribution and therefore permits the determination of an effective MFP, l_{eff} (equation (16)), without difficulties. The existence of an effective MFP in polycrystalline metals has been discussed for a long time. Landauer was among the first to put forward arguments [1] that denied the effective MFP concept. Theoretical investigations [4–7] based on the Boltzmann equation supported this opinion because only limiting forms of the results for $l/D \to 0$ show separate contributions to the total resistivity. Experimental data are obtained with various methods and fitted to or interpreted with different models. As far as our simplified considerations are applicable to polycrystalline metals, an effective MFP can be defined according to equation (16) for sufficiently spaced ($\exp(-D/l) \ll 1$) grain boundaries of arbitrary strength, and our method offers, in retrospect, a relatively transparent derivation of it. In experiments with coarse-grained ($D > l$) metals [12] a linear relationship between σ^{-1} and D^{-1} has been found.

As long as the distance between successive defect planes is greater than some MFP, the propagating electrons are scattered in the background and enter the next obstacle with phases that are not determined by previous scattering events at grain boundaries. The planar defects act independently of each other and the exact value of the MFP on the electronic flow. If the distance decreases ($D \lesssim l$) the electrons become sensitive to the accurate relation between D, l and the wavelength λ because in this case coherent as well as incoherent waves undergo a multiple scattering process at defects. Consequently, Matthiessen's rule should be violated. The description of such systems, realized in fine-grained materials, seems to be very complicated. Analytically, even the treatment of partially coherent transmission through two barriers is difficult (see for example [14]). Numerically, only the simpler 1D problem was studied in [15]. Any classical transport theory that deals with the intensity of transmitted and reflected electrons is, in principle, unsuitable for the investigation of the case $D \lesssim l$.

The validity of our result can be extended in part to that range. Consider the case $T \simeq 1$. The MFP associated with grain boundaries only (second term on the right-hand side of equation (16) measures the distance between successive scattering events, i.e. reflections, at these defects and is roughly given by $D/(1-T) \gg D$. If we choose R small enough the relation $l \ll D/(1-T)$ holds and our formulae can be used. Explicitly, we derive, e.g. from equation (18a) for $T \simeq 1$

$$\sigma/\sigma_b \simeq 1 - (3l/2D)(1-T) \simeq T^{3l/2D}. \tag{19}$$

On the basis of a great number of experiments, Hoffmann and coworkers [15, 16] stated that the conductivity decreases exponentially with the number of grain boundaries per MFP, l/D, and proposed an expression similar to (19). We emphasize, however, that a conductivity behaviour according to (19) is not only for $T \simeq 1$ in sufficient agreement with experimental data in the range $l > D$.

Acknowledgment

I wish to thank Professor Dr R Lenk for many stimulating and productive discussions.

Appendix. Calculation of C from the integral equation

Similar to $\rho_{\rm ind}$, equations (7) and (8), we combine the phase-compensating terms of the integral in (2) to

$$(\operatorname{Im} k^2/\operatorname{Im} G_b) \int_+ \mathrm{d}z'\, \delta\rho(z') \int \mathrm{d}A' \{|G_b^+|^2[1 - 2\,T(\theta_+)] + |G_b^-|^2\}. \tag{A1}$$

The total density is an odd function, $\delta\rho(z) = -\delta\rho(-z)$, whereas $\int \mathrm{d}A'\{\ldots\}$ represents even functions of the arguments $(z \pm z')$. In this case the (1D) Fourier-transformed expressions of the half-space integral (A1) can be factorized. In the light of the above, one can write the Fourier-transformed equation (2) as

$$\rho_{\rm ind}(q) = \delta\rho(q)[1 - F(q)] \tag{A2}$$

where $F(q)$ is assigned to the reduced integral kernel $(\operatorname{Im} k^2/\operatorname{Im} G_b)\int \mathrm{d}A'\,|G|^2$. To compute the magnitude C (11) we only consider the range $q \simeq 0$ and replace $\delta\rho(q)$ in (A2) by its long-wave part $\delta\rho^{\rm long}$. It is well known that the long-wave component is responsible for the asymptotic behaviour in real space, i.e. $\delta\rho^{\rm long}$ corresponds to

$\delta\rho(|z| \gg l)$, which is given in equation (11). In addition, for odd and exponentially localized functions, $f(z)$, the approximation

$$f(q) = \int_{-\infty}^{\infty} \mathrm{d}z \exp(\mathrm{i}qz) f(z) = \int_{-\infty}^{\infty} \mathrm{d}z\,(1 + \mathrm{i}qz \pm \ldots) f(z) \underset{q \simeq 0}{\rightarrow} \mathrm{i}q \int_{-\infty}^{\infty} \mathrm{d}z\, z f(z) = \mathrm{i}qp[f] \tag{A3}$$

holds. Applying (A3) to (A2) where $\delta\rho^{\mathrm{long}}(q)F(q)$ is retransformed into an integral and $\delta\rho^{\mathrm{long}}$ is substituted in real space by $C\,\mathrm{sgn}(z)$ (11) leads to equation (12).

References

[1] Landauer R 1957 *IBM J. Res. Dev.* **1** 223; 1970 *Phil. Mag.* **21** 863
[2] Lenk R 1990 *Phys. Status Solidi* b **161** 797
[3] Sommerfeld A and Bethe H 1933 *Handbuch der Physik* 2nd edn, vol 24, part 2 (Berlin: Springer) p 466
[4] Mayadas A F and Shatzkes M 1970 *Phys. Rev.* B **1** 1382
[5] Pichard C R, Tellier C R and Tosser A J 1979 *Thin Solid Films* **62** 189
[6] Warkusz F 1988 *Thin Solid Films* **161** 1
[7] Szszyrbowski J and Schmalzbauer K 1986 *J. Phys. F: Met. Phys.* **16** 2079
[8] Sorbello R S 1988 *Phys. Rev.* B **39** 4984
[9] Lenk R 1990 *Phys. Status Solidi* b **158** 653
[10] Lenk R 1989 *Phys. Status Solidi* b **154** 733
[11] Lenk R 1989 *Phys. Status Solidi* b **155** 627
[12] Kwabuliński P, Rasek J and Gierak Z 1988 *Phys. Status Solidi* a **107** 299
Kwabuliński P, Rasek J and Moroń J W 1985 *Phys. Status Solidi* a **88** 561
[13] Kirtley J R, Washburn S and Brady M J 1988 *Phys. Rev. Lett.* **60** 1546
[14] Büttiker M 1988 *IBM J. Res. Dev.* **32** 63
[15] Reiss G, Vancea J and Hoffmann H 1986 *Phys. Rev. Lett.* **56** 2100
[16] Vancea J, Hoffmann H and Kastner K 1984 *Thin Solid Films* **121** 201
[17] Reif F 1987 *Statistische Physik und Theorie der Wärme* 3rd edn (New York: de Gruyter) p 453